China Ocean Engineering, Vol.20, No.2, pp.243 – 258

Modelling of Random Waves over Submerged Breakwaters and Its Application to Reflection Estimation*

SHIH Ruey-Syan (石瑞祥)[a], CHOU Chung-Ren (周宗仁)[b,1] and YIM John-Z (尹　彰)[b]

[a] *Department of Civil Engineering, Tung Nan Institute of Technology, Taipei 22202, Taiwan, China*

[b] *Department of Harbour and River Engineering, National Taiwan Ocean University, Keelung 20224, Taiwan, China*

(Received 8 November 2005; accepted 20 January 2006)

ABSTRACT

Reflection and transmission of random waves from submerged obstacles under various conditions are investigated in this study by means of the boundary element method. The algorithm is based on the Lagrangian description with finite difference adopted for the approximation of time derivative. The accuracy of the model is confirmed by a previous study of the transmission of irregular waves in a water tank without any obstacle, under which sets of submerged breakwaters are located. To reduce the effect of reflection from the wall, a sponge zone is employed at the other end of the flume as an artificial absorbing beach. The power spectrum of Bretschneider-Mitsuyasu type defined by significant wave height, $H_{1/3}$, and period, $T_{1/3}$, is employed for the condition of incident waves chosen for the generation of irregular waves. Time histories of water elevations are measured with numerous pseudo wave gages on the free water surface. With reference to the method for the estimation of irregular incident and reflected waves in random sea presented by Goda and Suzuki (1976), the dissipation efficiency of the breakwaters is investigated. Gauges in different positions are tested for their suitability for the estimation of reflection coefficients for irregular waves. The present results demonstrate the effectiveness of the estimation of reflection coefficient for random waves, and indicate the feasibility of the numerical model.

Key words: *boundary element method*; *numerical wave tank*; *reflection coefficient*; *irregular wave*; *submerged obstacle*

1. Introduction

Great efforts have been devoted to the protection of coastal areas over many years by erecting dikes, seawalls, groin systems, and detached breakwaters. The sea walls, jetties, detached breakwaters, etc. are traditionally adopted as absorbing facilities for the dissipation of water wave energy. In Taiwan, starting from around the 80's, the construction of coastal jetties and detached breakwaters was progressively adopted for coastal protection. Previously, considerable quantities of armor units were piled up outside the protecting embankment for the efficiency of absorptions. That practice actually accomplished the purpose and ensured inland safty; however, it destroyed the landscape and ecological environment. In view of the preservation of natural landscape and the enforcement of so-called "amenity-oriented policy", recently, many constructions are being substituted by ecological engineering method. Modifications such as submerged breakwaters, artificial submerged reefs, artificial beaches, amenity-oriented sea dykes, etc., can now be found by the seashore. The adoptation of submerged

* The work was financially supported by the Science Council (Project No. NSC-92-2611-E-236-001)

1 Corresponding author. E-mail: rsshih@mail.tnit.edu.tw

breakwaters may not only help decrease the damage to the landscape, but also force waves to break either above or behind the obstacles. Physical model experiments are usually adopted in an everwidening range of engineering investigations, and numerical models are themselves conditioned by the requirements of the experimental measurements. In virtue of the rapid development of science and technology of electronic computer nowadays, numerous numerical models are being established for the estimation of oceanic physical characteristics, and providing reliable statistics for the design and construction of coastal structures. The investigation of irregular waves propagating over a set of submerged obstacles in various positions is performed in this study by means of the boundary element method. The dissipation of wave energy by submerged obstacles has been extensively investigated by many researchers, e.g., an experimental investigation on the submerged dike was presented by Nakamura *et al*. (2001), which mainly deals with the damping effect due to breaking on the submerged dike. The probability density function of the wave heights and periods as well as the shape of the spectrum was discussed by Lee and Black (1978) using spectral analysis and zero-up-crossing procedure.

Regarding the estimation of reflection coefficients, a well known method presented by Goda and Suzuki (1976) to resolve the incident and reflected waves from the records of composite waves in a random wave field has been extensively adopted as a way to estimate the reflection coefficient in laboratory, where the water elevation is measured by a two-probe system. The incident and reflected spectra are calculated by a least square method presented by Mansard and Funke (1980) using the data of a simultaneous measurement of water elevation by three probes. Similary, Gaillard *et al*. (1980) published a method of evaluation of both the incident and reflected wave spectra in laboratory experiments and/or field investigation by use of the analysis of wave records obtained by a three-probe array, and their results are also found to be reliable. Based on the use of digital filters, Frigaard and Brorsen (1995) presented a new method for separating irregular waves into incident and reflected waves, and the efficiency of the model was demonstrated by both physical and numerical tests. The above method was modified later by Baldock and Simmonds (1999) to account for normally incident linear waves propagating over a sloping bathymetry, whose amplitude and phase change between two probes was determined with the linear shoaling theory.

The estimation of reflection coefficients in a wave flume through measurement of water evaluations with three probes was studied by Sanchez (2000) using a complex function. Shu *et al*. (2001) developed a model that predicts the reflections for irregular waves normally incident upon a perforated-wall caisson breakwater by using an eigenfunction expansion method. Considering the influence of a bounded beach, Doclos and Clément (2003) presented a method for the estimation of transmission and reflection coefficients for water waves in a small basin by extending the Goda two-probe method to three probes.

Numerical simulation of the generation and propagation of irregular waves in a 2D wave flume has been investigated by Chou *et al*. since 1998, and the numerical scheme has been improved by employment of a sponge zone at the end of the flume (Chou *et al*., 2001) to eliminate the reflected waves. And the generation of irregular waves revealed that the improved numerical scheme is capable of de-

scribing the propagation of irregular waves satisfactorily (Shih *et al.*, 2004). In this paper, the deformation of irregular waves over submerged obstacles and its application to reflection coefficient estimation are investigated.

2. Theoretical Formulations

2.1 Basic Assumptions and Governing Equations

The numerical wave flume is confined by a piston type wave generator located at the right, Γ_1, an undisturbed free water surface, Γ_2, an impermeable vertical wall, Γ_3, an impermeable bottom floor, Γ_4, and an impermeable submerged obstacle, Γ_5, as shown schematically in Fig. 1. The boundaries are discretized to linear elements. The origin of the coordinate system is located on the still water surface with the z-axis pointing positively upwards and the x-axis pointing positively rightwards. The vertical wall is adopted at the left end of the flume so as to bear more resemblance to the physical wave generation. The fluid within the region is conventionally assumed as incompressible, inviscid, and irrotational; hence, the velocity potential $\Phi(x, z, t)$ satisfies the following Laplace equation:

$$\frac{\partial^2 \Phi}{\partial x^2} + \frac{\partial^2 \Phi}{\partial z^2} = 0. \tag{1}$$

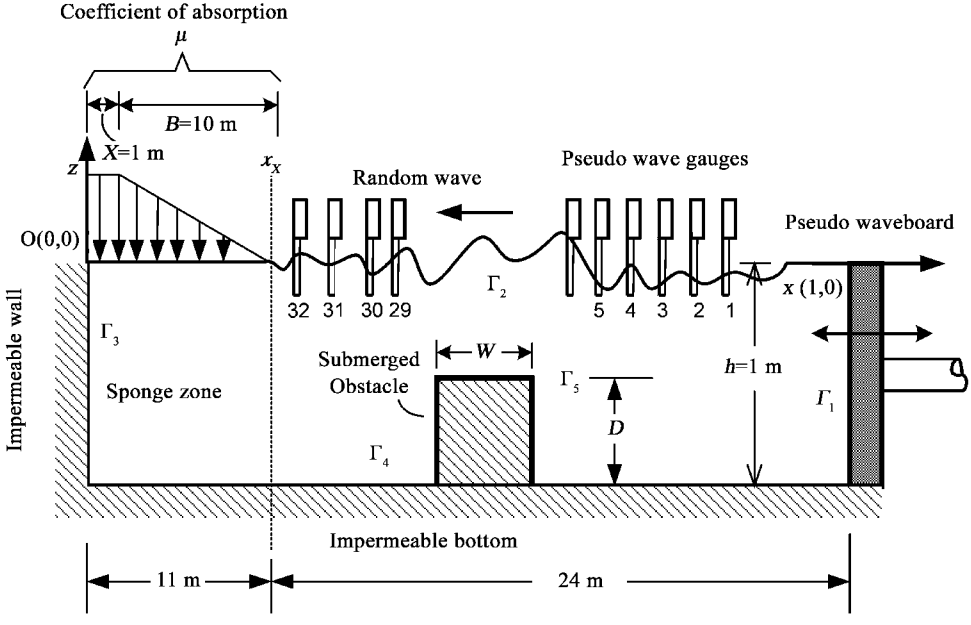

Fig. 1. Definition sketch of numerical wave flume comprises pseudo wave gauges, submerged obstacle and absorbing technique.

The boundary conditions on the undisturbed free water surface can be obtained from nonlinear kinematic and dynamic conditions, and can be express in the following Lagrangian form:

$$u = \frac{\mathrm{D}x}{\mathrm{D}t} = \frac{\partial \Phi}{\partial x}; \tag{2}$$

$$w = \frac{\mathrm{D}z}{\mathrm{D}t} = \frac{\partial \Phi}{\partial z}; \tag{3}$$

$$\frac{\mathrm{D}\Phi}{\mathrm{D}t} + g\zeta - \frac{1}{2}\left[\left(\frac{\partial \Phi}{\partial x}\right)^2 + \left(\frac{\partial \Phi}{\partial z}\right)^2\right] + \frac{P}{\rho} = 0; \tag{4}$$

where, u and w are the horizontal and vertical components of the water particle velocity; $\mathrm{D}(\ )$ is the Lagrangian derivative; g is the gravitational acceleration, with ζ representing the surface fluctuation; ρ is the density of water; P is the gage pressure on the water surface, and is assumed to be constant (i.e. $P = 0$) for the non-absorbing area.

The absorption of free surface waves including various conditions is discussed by Cao *et al.* (1993). In the present research, the value of the pressure term, P, is defined proportional to the potential on the free water surface, thus, $P(x, \zeta)$ is expressed as:

$$P(x, \zeta) = \mu(x)\Phi(\xi, \eta, t) \tag{5}$$

where, $\mu(x)$ is the beach absorption function, which is assumed to vary smoothly along section $x_X - x_B$, but remains constant after x_X; the coefficient of absorption can thus be expressed as:

$$\mu(x, t) = \mu_0(t)\rho\left(\frac{x_B - x}{B}\right)^{\alpha}, \quad x_X < x < x_B \tag{6}$$

$$\mu(x, t) = \mu_0(t)\rho, \quad x \leqslant x_X \tag{7}$$

in which, $B = x_X - x_B$ is the length of varying-value section. As can be seen from Fig. 1, a linear absorption parameter is adopted in this paper, i.e. $\alpha = 1$.

By matching the horizontal velocity $U(t)$ of the paddle and that of the fluid, the boundary condition on the wave-paddle is obtained through the following association:

$$\bar{\Phi} = \frac{\partial \Phi}{\partial n} = -U(t), \quad \text{on} \quad \Gamma_1, \tag{8}$$

where, n is the unit outward normal vector; since the Bretschneider-Mitsuyasu spectrum is used as the target spectrum for the generation of irregular waves, the value of $U(t)$ is equal to the horizontal velocity and the boundary condition on the wave-paddle, i.e. Eq. (8), is

$$U(t) = \sum_{n=1}^{N} \sqrt{2\,df S_0(f_n)}\,\alpha(f)\,\sigma_n \cos(\sigma_n t - \varepsilon_n) \tag{9}$$

in which, $\sigma_n = 2\pi f_n$, $\alpha(f)$ denotes the transfer function, $S_0(f_n)$ is the spectrum, f is the frequency, ε_n the random variable number between $0 \sim 2\pi$, and N the total number of sampling, respectively. Expatiations on the generation of random waves are discussed in Shih *et al.* (2004).

Inasmuch as the particle velocity is null in the normal direction on the impermeable vertical wall, the bottom floor, and the submerged obstacle, the conditions are therefore prescribed as:

$$\frac{\partial \Phi}{\partial n} = 0, \quad \text{on} \quad \Gamma_3, \Gamma_4 \quad \text{and} \quad \Gamma_5. \tag{10}$$

2.2 Governing Equation and Boundary Discretization

According to Green's second identity, the continuity equation in differential form, Eq. (1), can thus be transformed into a boundary integral equation:

$$c\Phi(x,z;t) = \frac{1}{2\pi}\int_{\Gamma}\left\{\frac{\partial\Phi(\xi,\eta;t)}{\partial n}\ln\left(\frac{1}{r}\right) - \Phi(\xi,\eta;t)\frac{\partial}{\partial n}\left[\ln\left(\frac{1}{r}\right)\right]\right\}\mathrm{d}s \tag{11}$$

$$c = \begin{cases} 1 & \text{inside the fluid domain} \\ 1/2 & \text{on the smooth boundary} \\ 0 & \text{outside the fluid domain} \end{cases}$$

where $r = \sqrt{(\xi - x)^2 + (\eta - z)^2}$.

The boundaries, $\Gamma_1 \sim \Gamma_5$, are divided into $N_1 \sim N_5$ discrete linear elements, respectively, i.e. 10 elements for the pseudo wave-paddle, 234 elements for the free water surface, 5 elements for the vertical wall, 70 elements for the impermeable bottom, and 5 elements for each side of the impermeable submerged obstacle. The discretization schemes were discussed in the analyses to test the effects of the mesh sizes Δx by Shih *et al*. (2004). On that basis, Eq. (11) can be expressed in the following matrix form:

$$[\Phi_i] = [O_{ij}][\bar{\Phi}_i]\ ;\quad i,j = 1 \sim 5 \tag{12}$$

where, $[\Phi]$ and $[\bar{\Phi}]$ are, the velocity potential and its associated normal derivative, respectively,. The coefficients of the matrix $[O]$ are related to the geometric shapes of the boundaries.

The positions of nodes are regridded at every time step; thus, the new positions of the free water surface, (x^{k+1}, z^{k+1}) can be obtained by differentiating the time derivatives in Eqs. (2), (3), and (4) through forward differencing:

$$x^{k+1} = x^k + \left(\frac{\partial\Phi_2^k}{\partial x}\right)\Delta t\ ; \tag{13}$$

$$z^{k+1} = z^k + \left(\frac{\partial\Phi_2^k}{\partial z}\right)\Delta t. \tag{14}$$

The velocity potential on the free water surface at the next time step, $t = (k+1)\Delta t$ is given by:

$$\Phi_2^{k+1} = \Phi_2^k + \frac{1}{2}\left[\left(\frac{\partial\Phi_2}{\partial s}\right)^2 + \left(\frac{\partial\Phi_2}{\partial n}\right)^2\right]\Delta t - gz^{k+1}\Delta t - \frac{P^k}{\rho}\Delta t \tag{15}$$

where s and n denote, respectively, the tangential and the normal direction. The normal derivatives on the boundaries Γ_1, Γ_3, Γ_4 and Γ_5 at $t = (k+1)\Delta t$ can thus be obtained by the use of Eqs. (8) and (10) written more compactly as:

$$\begin{bmatrix}\Phi_1\\ \bar{\Phi}_2\\ \Phi_3\\ \Phi_4\\ \Phi_5\end{bmatrix}^{k+1} = \begin{bmatrix}\boldsymbol{I} & -O_{12} & 0 & 0 & 0\\ 0 & -O_{22} & 0 & 0 & 0\\ 0 & -O_{32} & \boldsymbol{I} & 0 & 0\\ 0 & -O_{42} & 0 & \boldsymbol{I} & 0\\ 0 & -O_{52} & 0 & 0 & \boldsymbol{I}\end{bmatrix}^{-1}\begin{bmatrix}O_{11} & 0 & O_{13} & O_{14} & O_{15}\\ O_{21} & -\boldsymbol{I} & O_{23} & O_{24} & O_{25}\\ O_{31} & 0 & O_{33} & O_{34} & O_{35}\\ O_{41} & 0 & O_{43} & O_{44} & O_{45}\\ O_{51} & 0 & O_{53} & O_{54} & O_{55}\end{bmatrix}\begin{bmatrix}\bar{\Phi}_1\\ \Phi_2\\ \bar{\Phi}_3\\ \bar{\Phi}_4\\ \bar{\Phi}_5\end{bmatrix}^{k+1} \tag{16}$$

where $\boldsymbol{I}$ is the identity matrix. Detailed description concerning the iterative scheme of time stepping and computational procedures can be found in Chou and Shih (1996), the stability of the numerical scheme depending on the Courant number discussed in Chou *et al*. (2001).

2.3 Estimation of Reflection Coefficient, K_r

For the determination of the reflection coefficient of irregular waves, the estimation of wave reflection through the separation of incident and reflected waves in a random wave field has been extensively investigated. e.g. a widely used method was presented by Goda and Suzuki (1976) for the estimation of incident and reflected waves in a random wave field in frequency domain, and this method was further improved by Mansard and Funke (1980) using least square techniques. A time-domain method for the separation of irregular waves by the use of digital filters was investigated by Frigaard and Brorsen (1995), and the method is able to separate the wave fields in real time. The reflection coefficients of irregular waves are estimated in this study utilizing the method of Goda and Suzuki (1976). Based on the time histories of water elevations measured with numerous pseudo wave gages on the free water surface, the amplitude is analyzed with the FFT technique, consequently, and then the reflection coefficients are estimated as follows.

The composite wave profiles of incident and reflected waves at locations $x = x_1$ and $x = x_1 + \Delta l$ can be expressed as:

$$\eta_1 = (\eta_i + \eta_r)_{x = x1} = A_1\cos\sigma t + B_1\sin\sigma t; \tag{17}$$

$$\begin{cases} A_1 = a_i\cos\theta_i + a_r\cos\theta_r \\ B_1 = a_i\sin\theta_i + a_r\sin\theta_r \end{cases}; \tag{18}$$

$$\eta_2 = (\eta_i + \eta_r)_{x = x1+\Delta l} = A_2\cos\sigma t + B_2\sin\sigma t; \tag{19}$$

$$\begin{cases} A_2 = a_i\cos(\theta_i + k\Delta l) + a_r\cos(\theta_r + k\Delta l) \\ B_2 = a_i\sin(\theta_i + k\Delta l) + a_r\sin(\theta_r + k\Delta l) \end{cases}; \tag{20}$$

where, $\theta_i = kx_1 + \varepsilon_i$ and $\theta_r = kx_1 + \varepsilon_r$, ε being the phase angle; k is the wave number; σ is the angular frequency; subscripts "i" and "r" denote, respectively, the incident and reflected waves; Δl is the spacing between two measuring probes.

The amplitudes a_i and a_r can thus be calculated by:

$$a_i = \frac{1}{2\,|\sin k\Delta l\,|}\left[(A_2 - A_1\cos k\Delta l - B_1\sin k\Delta l)^2 + (B_2 + A_1\sin k\Delta l - B_1\cos k\Delta l)^2\right]^{1/2}; \tag{21}$$

$$a_r = \frac{1}{2\,|\sin k\Delta l\,|}\left[(A_2 - A_1\cos k\Delta l + B_1\sin k\Delta l)^2 + (B_2 - A_1\sin k\Delta l - B_1\cos k\Delta l)^2\right]^{1/2}. \tag{22}$$

The energies of the incident and reflected waves, E_i and E_r, could be obtained from:

$$E_i = \int_{f_{\min}}^{f_{\max}} S_i(f)\,\mathrm{d}f; \tag{23}$$

$$E_r = \int_{f_{\min}}^{f_{\max}} S_r(f)\,\mathrm{d}f. \tag{24}$$

Consequently, the reflection coefficient, K_r, can be estimated:

$$K_r = \sqrt{\frac{E_r}{E_i}}. \tag{25}$$

3. Results and Discussion

3.1 Absorption of Irregular Waves with Submerged Obstacles

The effectiveness of the artificial absorbing beach is demonstrated by Chou *et al*. (2002) in the simulations of both solitary and periodic waves. The same absorbing technique is employed represents here, i. e. a sponge zone at the end of the flume to minimize the reflection effects, and its efficiency of irregular wave absorption is discussed by Shih *et al*. (2004). However, the numerical model becomes much more complicated after a submerged obstacle is set: the reflected waves caused by the obstacle cannot be eliminated by the absorbing technique as it is placed at the end of the flume, and then they will inevitably contaminate the incident wave train, including the re-reflection from the wave paddle. The repeated process may cause great errors to the estimations; furthermore, the flume adopted presently is 35 m in length, while the longest wave may be up to 13 m according to the selected period (0.5 ~ 0.45 sec), indicating that the length of the flume is less than 3 complete "maximum wavelengths". Owing to the reflections and the limited length of the flume, only wave data for a short period are available for analysis, e.g. the quantity of total sampling data for simulation is about 1549 (approximately 38.7 sec) for $T_{1/3} = 0.8$ sec and decreases to 1186 (approximately 29.65 sec) for $T_{1/3} = 1.0$ sec. This may greatly affect the accuracy of the results. This problem could be rudimentarily solved by lengthening the flume, or by a more effective technique: developing the present wave paddle into a so-called "absorbing wave maker", which will be discussed in the future.

3.2 Reflections due to Waveform Determination

The time series of waveform variations for identical duration are shown in Fig. 2(a) ~ (d), where the significant wave period of incident wave and the height of submerged dike are $T_{1/3} = 1.0$ sec and $D = 0.5h$, respectively, whereas the width of the dike increases gradually from $W = 1h \sim 4h$. As revealed in Fig. 2(d), when the width W reaches $4h$, the wave height distributions behind the dike show a appeared lower range than those shown in Fig. 2(a) ~ (c). Unlike monochromatic waves with stationary frequency, irregular waves are composed of considerable quantities of component waves with different frequencies and heights; partial standing waves apparently form in front of the breakwater at the location around $x = 23$ m, and, since the state of incident waves remains unchanged, the formation of partial standing waves may as well denote the increase of reflected waves by waveform determination. However, the appearance of "Node" and "Antinode" in the wave crest envelope is unapparent and mostly never occurs in random wave; therefore, estimation of the quantity of reflected wave energy cannot be done through waveform determination for different significant wave periods $T_{1/3}$ as it is in Fig. 2, i.e. the intensity of partial standing waves does not represent reflection quantities. Concerning this problem, Fig. 3(a) ~ (i) shows the case with varying significant wave periods $T_{1/3}$ from 0.6 sec to 1.4 sec, where the width and height of the submerged dike are $W = 4h$ and $D = 0.5h$ respectively.

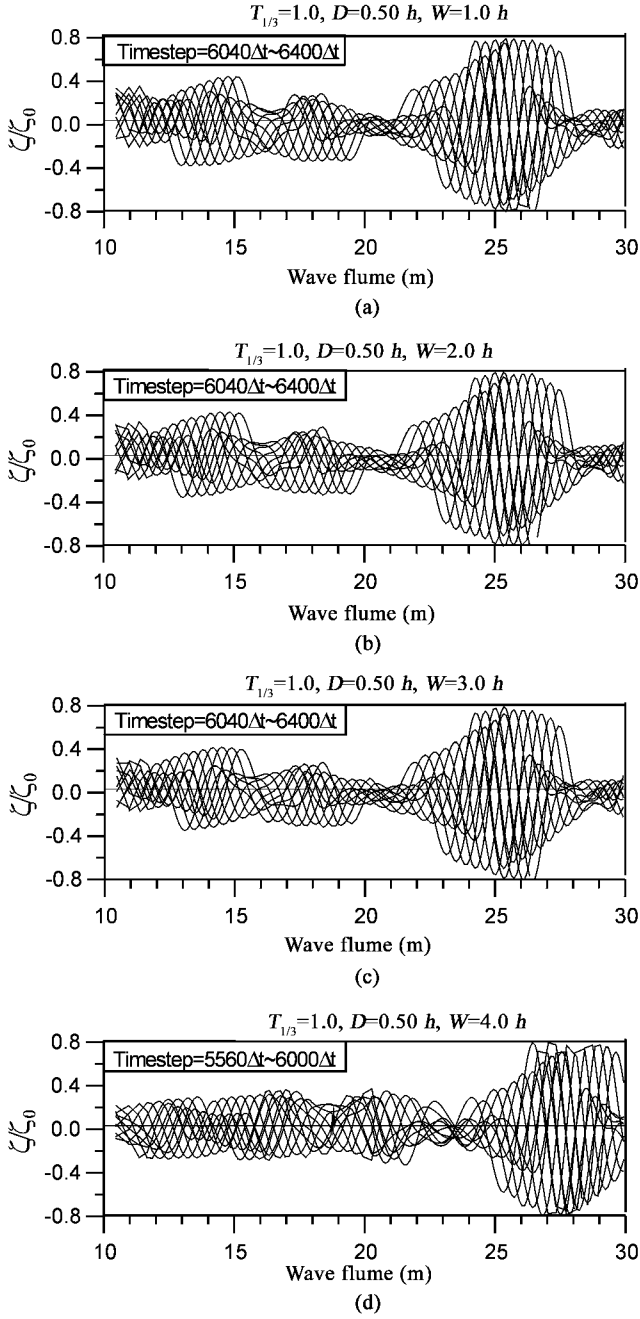

Fig. 2. Time histories of water elevations due to submerged obstacles with various widths, W ($T_{1/3}=1.0$, $D=0.5h$, $\zeta_0=\frac{1}{2}H_{1/3}$).

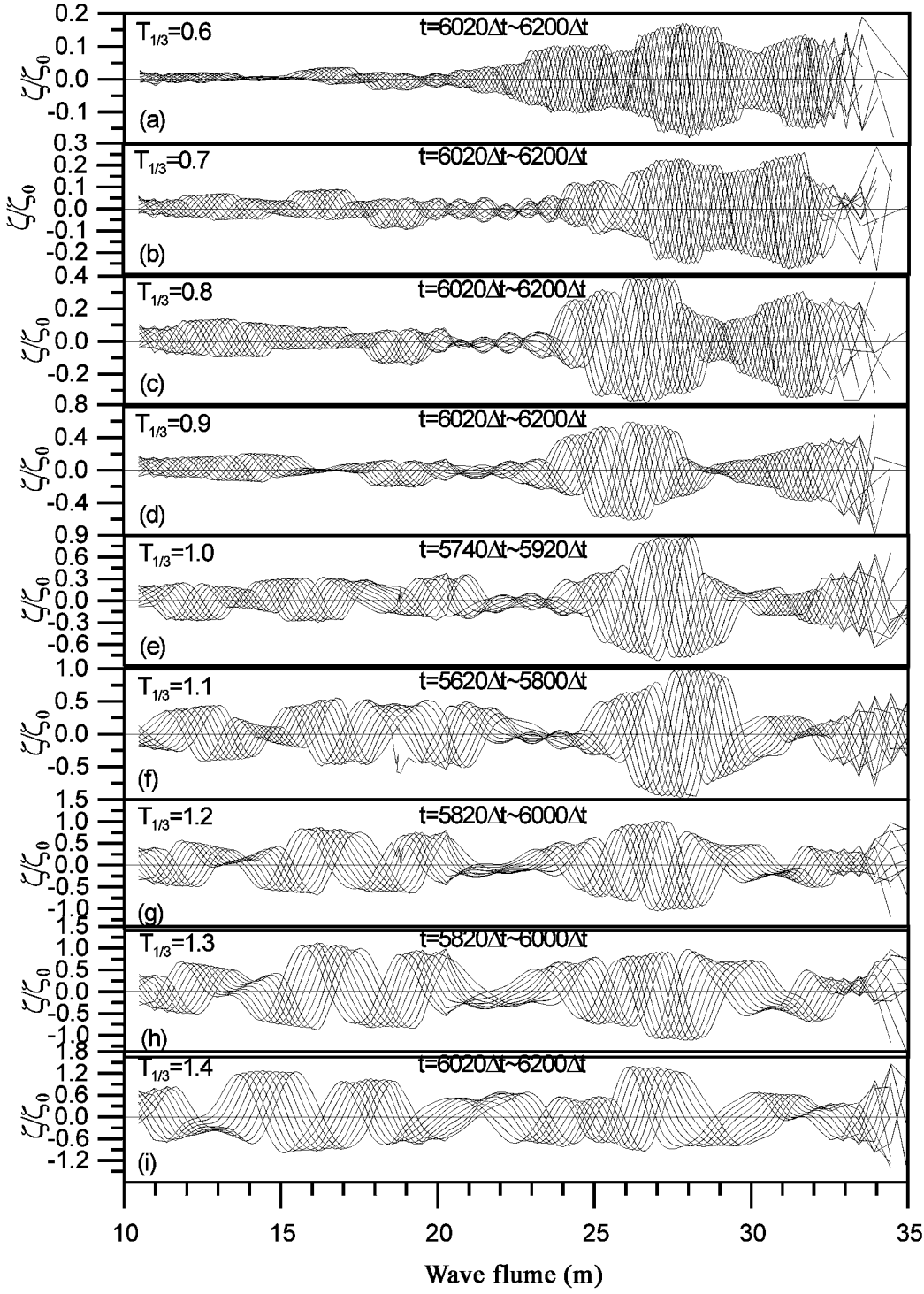

Fig. 3. Comparison of time histories of water elevations due to submerged obstacles. ($D = 0.5h$, $W = 4h$, $\zeta_0 = \frac{1}{2} H_{1/3}$)

As revealed, the partial standing waves in front of the dike are conspicuous for $T_{1/3} = 0.6 \sim 1.0$ sec, but rather inconspicous for other values. Since the wave height distributions behind the dike does not seem to decrease substantially as it is expected, it is conceivable that the reflected waves are mainly component waves with short periods while waves with longer periods pass over the submerged dike. According to Fig. 4, when the width W increases up to $3h$ and the height D remains unchanged ($= 0.75h$), waves will travel a longer distance over the obstacle and thus will have a greater shoaling effect. This may in fact lead to wave breaking, as shown in the figure for $x = 18 \sim 20$ m. This phenomenon is also found in our physical model test in a wave flume, as shown in Fig. 5, which is reversed left and right for comparison with Fig. 4. The wave damping effect of the submerged dike with wave breaking is remarkably different from that in non-breaking cases; nevertheless, the simulation of breaking of irregular waves is still impossible and so far not considered in this paper. To illustrate the above occurrences, the spectral densities measured in front of and behind the obstacle are shown in Fig. 6(a) ~ (d), from which one can find that, in the case of $T_{1/3} = 1.2$ sec, the reflection seems to be the largest. This will be discussed in the following section for various obstacle conditions.

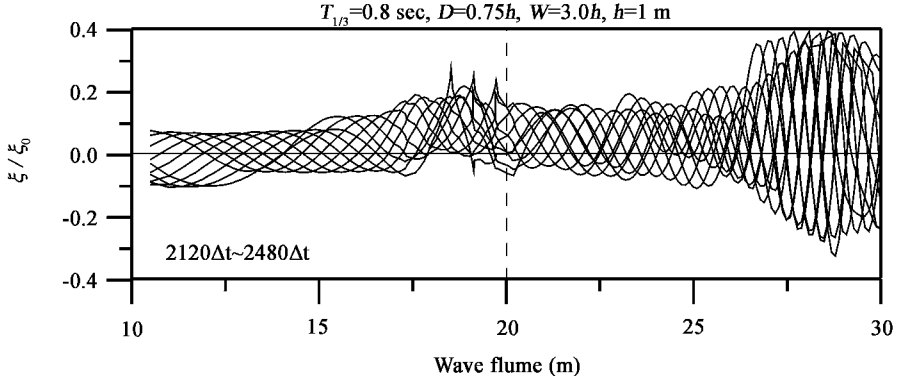

Fig. 4. Time histories of water elevations due probably to shoaling by submerged obstacles. ($\zeta_0 = \frac{1}{2} H_{1/3}$)

3.3 Determination of Reflection Coefficient

The reflection coefficient is determined with the two-gauge analysis technique of Goda and Suzuki (1976) from the variations of water elevation. The time histories of surface elevation are measured with a total of 32 pseudo wave gauges, and starting from the wave-paddle, Stations 1 ~ 32 are used to record the developments of irregular waves along the wave tank. Table 1 lists the number of all stations and their distances from the origin. Though the wave gauges may be located as near as $0.2L$ (L stands for wavelength) to the obstacle in regular wave tests, it was recommended by Goda and Suzuki (1976) to be located at a distance of at least more than one wavelength, L, from both the obstacle and the paddel in irregular wave tests. It is known that the wavelength of irregular wave consists of multiple components; accordingly, the gauges are combined and distributed to twelve groups as listed in Table 2, and

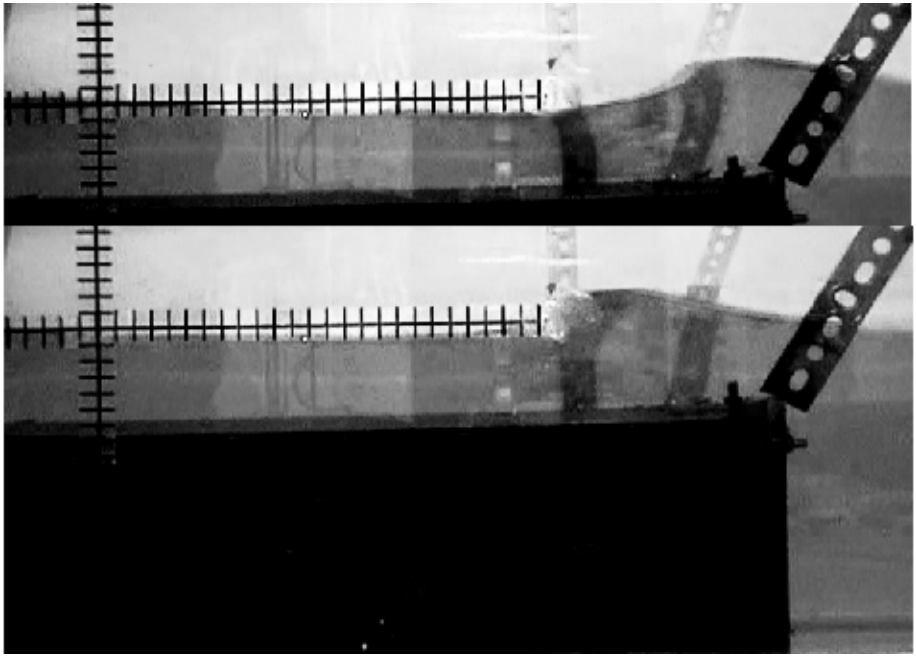

Fig. 5. Wave breaking due to shoaling by submerged obstacles. ($T_{1/3} = 0.4$ sec, $D = 0.75h$, $W = 3.0h$, $h = 0.25$ m)

the spacing between every two adjacent gauges is $\Delta l = 0.5h$. Fig. 7 shows the estimated results from various combinations of wave gauges with different positions. Most of the results are concentrated in a small ambit, as circled; some show large discrepancies, indicating inappropriate grouping (gauge location), and are then pruned away in analysis. Inappropriate gauge grouping should be avoided in laboratory physical model test.

Table 1 Location of wave gauges along the flume

Gauge No.	Location (m)	Gauge No.	Location (m)	Gauge No.	Location (m)	Gauge No.	Location (m)
01	31.0	09	22.7	17	21.9	25	21.1
02	29.0	10	22.6	18	21.8	26	20.0
03	26.0	11	22.5	19	21.7	27	19.0
04	25.0	12	22.4	20	21.6	28	18.0
05	24.0	13	22.3	21	21.5	29	17.0
06	23.0	14	22.2	22	21.4	30	15.0
07	22.9	15	22.1	23	21.3	31	12.0
08	22.8	16	22.0	24	21.2	32	11.0

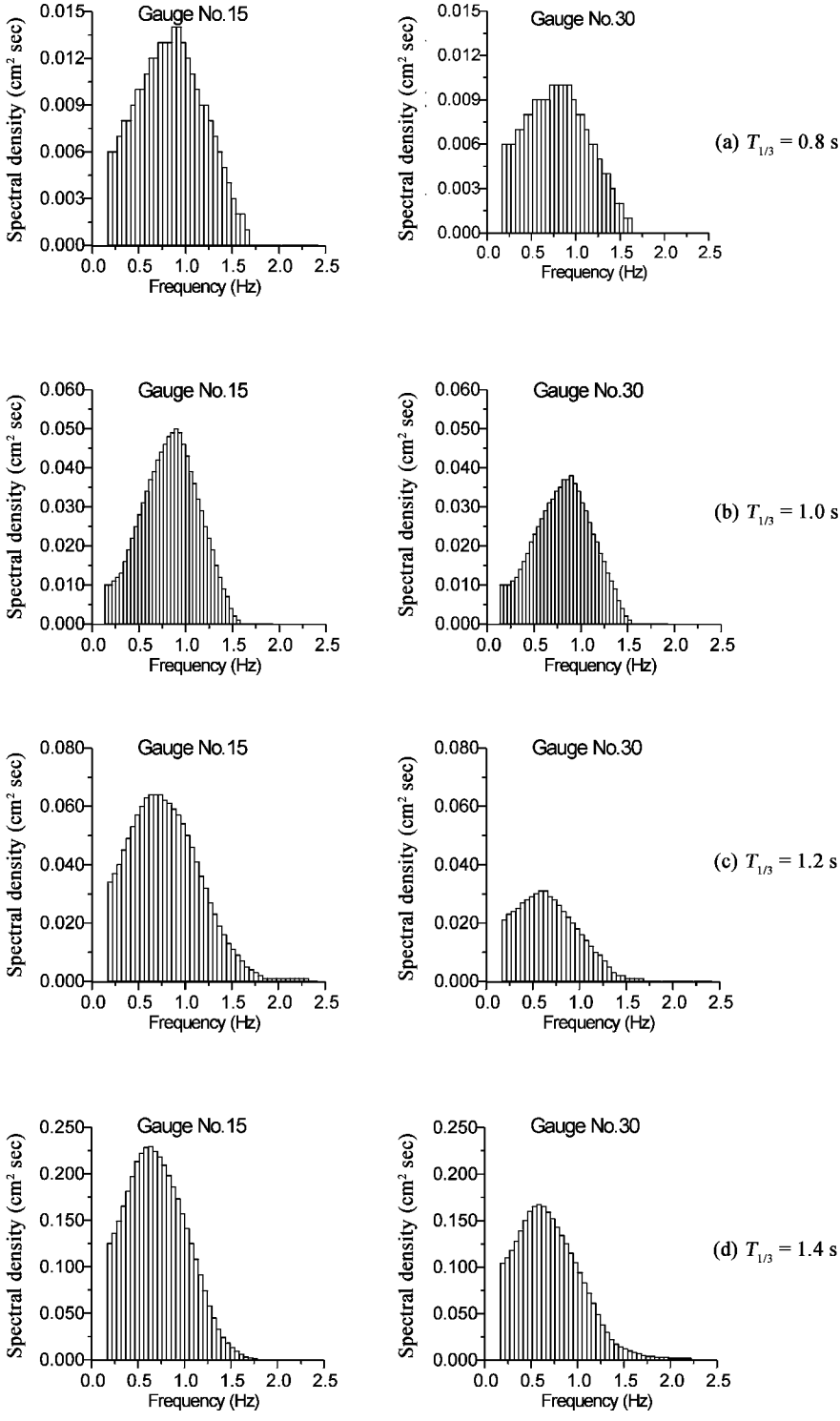

Fig. 6. Spectra of irregular waves measured before (gauge No.15) and after (gauge No.30) the obstacle. (D = 0.50h, W = 4h)

Table 2 Combination of wave gauges

Group No.	Gauge No. ($\Delta l = 0.5h$)		Group No.	Gauge No. ($\Delta l = 0.5h$)	
A	19	14	G	13	08
B	18	13	H	12	07
C	17	12	I	11	06
D	16	11	J	10	05
E	15	10	K	09	04
F	14	09	L	08	03

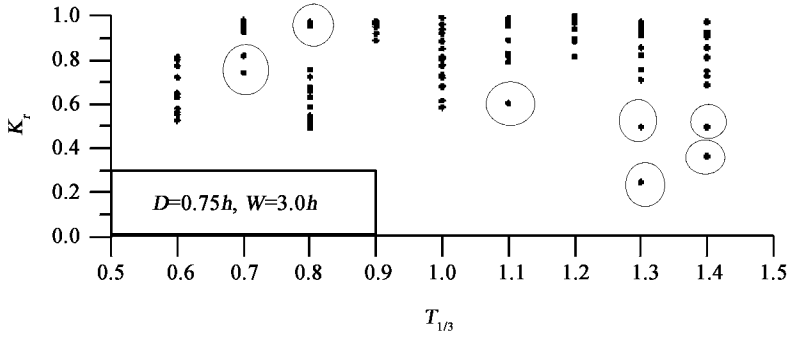

Fig. 7. Estimated results by various combinations of wave gauges with different positions.

As mentioned previously, after the submerged obstacle is placed, the waves reflected by the obstacle travel back to the paddle and are re-reflected; these re-reflected waves propagate toward the obstacle and are reflected again. The process may be repeated several times until the simulation is halted by accumulated errors. Therefore, the sampling time of data for reflection analysis applied here is equivalent to the experimental measurement adopted practically in laboratory, i.e. the sampling starts when the reflected waves from the obstacle reaches the gauges, and concludes before the re-reflected wave from the paddle approaches. Though Duclos and Clément (2003) have presented a new method for the calculation of reflection coefficient in a small basin by extending Goda and Suzuki's method to three-probe technique, still, the Goda method is utilized in prexent study.

The accuracy of the model is confirmed by comparison the numerical results with experimental results, as shown in Fig. 8. The physical model test was carried out in a 0.6 m × 0.8 m × 16 m wave flume at the Fluid Mechanics Laboratory of Tung Nan Institute of Technology, with a constant water depth of 0.25 m. Fig. 9(a) ~ (d) presents the variations of reflection coefficient for irregular waves passing over a submerged dike with identical width W. From the figure it can be found that, when $W \leqslant 2h$ and $T_{1/3} < 1.0$, the influence of D on Kr seems to be rather small, as shown in Fig. 9(a) and Fig. 9(b). Contrarily, as revealed in Fig. 9 (c) and Fig. 9 (d), except for the case of $T_{1/3} = 0.6$ sec and 0.8 sec with $W = 3h$, the reflection coefficient in its entirety apparently increases when $B > 2h$, particularly when the height of the dike D reaches $0.75h$. This can also be seen in Fig. 10(a)

~ (c) where the height of the submerged dike D remains identical. The increase of the dike's width influences the reflection slightly under the conditions of $D \leqslant 0.5h$ and $W \leqslant 2h$; nevertheless, the reflection coefficient increases to a relatively large degree with the width of the dike when $D = 0.75h$ and $W = 3h \sim 4h$. A comparison of Fig. 9 with Fig. 10 shows that the reflection coefficient for waves for $W = 3h$ and $D = 0.75h$ undulates and has larger or smaller values than that for waves with $T_{1/3} = 0.6 \sim 1.0$ sec, and it also seems to have the largest variations.

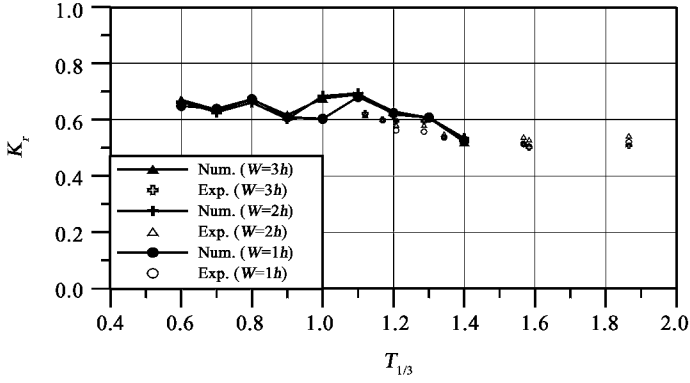

Fig. 8. Comparison of numerical and experimental results. ($D = 0.5h$)

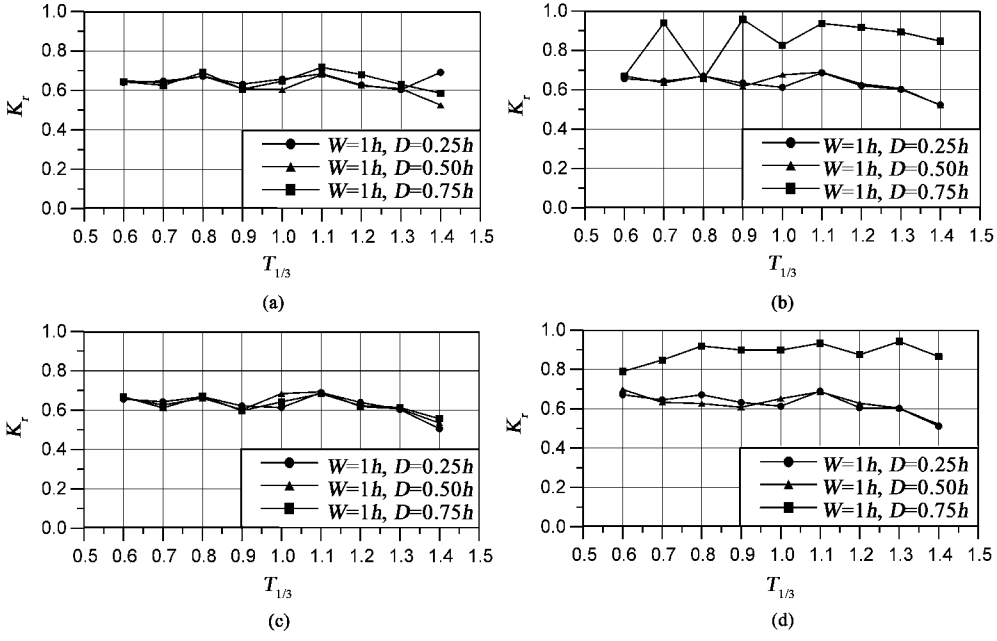

Fig. 9. Variations of reflection coefficients due to submerged obstacles for various combinations (W remains identical).

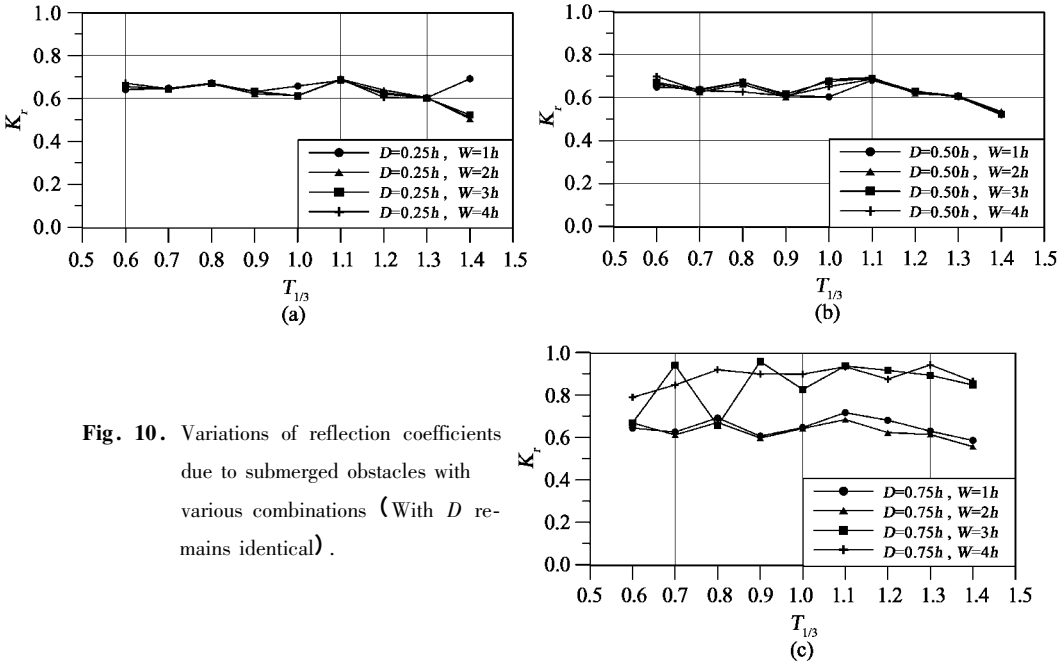

Fig. 10. Variations of reflection coefficients due to submerged obstacles with various combinations (With D remains identical).

4. Conclusions

The application of numerical wave flume to the study of irregular wave propagation and the estimation of reflection coefficient for irregular waves over submerged breakwaters under various conditions are investigated in this study by means of BEM. Some conclusions may be drawn from the present results.

(1) The present numerical scheme is applicable for the estimation of reflection coefficient, and the estimated results could be regarded as reference material before hydraulic experiments to economize on both the spatial and temporal expenditure.

(2) Most of the locations of wave gauges given herein for the estimation of wave reflection are suitable. Inappropriate locations of wave gauges may lead to large discrepancies in the estimation, and thus should be avoided. The reflection coefficient for each case is obtained by averaging the estimated results from each gauge group. Though small discrepancies may occur between each combination, the variation tendency in its entirety is in unanimity.

(3) The increase of the width of the dike influences the reflection coefficient slightly when $D \leqslant 0.5h$ and $W \leqslant 2h$; however, the reflection coefficient increases to a relatively large degree with the width of the dike when $D > 0.5h$ and $W > 2h$.

(4) Specifically, reflected waves caused by an obstacle is unable to be eliminated by the absorbing techniques employed at the end of the flume; they will travel back to the paddle and are re-reflected, and these re-reflected waves will be reflected again by the obstacle. The repeated process may cause great errors to the estimations. Therefore, in addition to the lengthening of the flume, development of the present wave paddle into a so-called "absorbing wave maker" should be considered.

References

Baldock, T. E. and Simmonds, D. J., 1999. Separation of incident and reflected waves over sloping bathymetry, *Coastal Engineering*, **38**(3): 167 ~ 176.

Cao, Y., Beck, R. F. and Schultz, W. W., 1993. An absorbing beach for numerical simulations of nonlinear waves in a wave tank, *Proc. 8th Int. Workshop Water and Floating Bodies*, 17 ~ 20.

Chou, C. R. and Ouyang, K., 1998. Development of numerical irregular wave making channel, *Proc. of the 8th China ~ Japan Symposium on Boundary Element Method*, Acadmic Publisher, 142 ~ 149.

Chou, C. R. and Shih, R. S., 1996. Generation and deformation of solitary waves, *China Ocean Engineering*, **10**(4): 419 ~ 432.

Chou, C. R., Shih, R. S. and Yim, Z. J., 2001. A numerical wave tank for nonlinear waves with passive absorption, *China Ocean Engineering*, **15**(2): 253 ~ 268.

Chou, C. R., Shih, R. S. and Yim, Z. J., 2002. Optimizing deployment of sponge zone on numerical wave channel, *Journal of the Chinese Institute of Engineers*, **25**(2): 147 ~ 156.

Duclos, G. and Clément, A. H., 2003. A new method for the calculation of transmission and reflection coefficients for water waves in a small basin, *Comptes Rendus Mecanique*, 331, 225 ~ 230.

Frigaard, P. and Brorsen, M., 1995. A time-domain method for separating incident and reflected irregular waves, *Coastal Enineering*, **24**(3-4): 205 ~ 215.

Gaillard, P., Gauthier, M. and Holly, F., 1980. Method of analysis of random wave experiments with reflecting coastal structures, *Proc. 17th Int. Conf. Coastal Eng.*, Sydney, 1, 204 ~ 220.

Goda, Y. and Suzuki, Y., 1976. Estimation of incident and reflected waves in random wave experiments, *Proc. 15th Int. Conf. Coastal Eng.*, Honolulu, 1, 828 ~ 845.

Lee, T. T. and Black, K. P., 1978. The energy spectra of surf waves on a corel reef, *Proc. 16th Int. Conf. Coastal Eng.*, 1, 588 ~ 608.

Mansard, E.P.D. and Funke, E. R., 1980. Method of analysis of random wave experiments with reflecting coastal structures, *Proc. 17th Int. Conf. Coastal Eng.*, Sydney, 1, 154 ~ 172.

Nakamura, N., Shiraishi, H. and Sasaki, Y., 1966. Wave damping effect of submerged dike, *Proc. 10th Int. Conf. Coastal Eng.*, 1, 254 ~ 267.

Sanchez, M., 2000. Estimation du coefficient de refléxion en canal à houle, *CR Acad Sci*, Paris t 328, Série Ⅱ b: 883 ~ 889.

Shih, R. S., Chou, C. R. and Yim, Z. J., 2004. Numerical Investigation on the Generation and Propagation of Irregular Waves in A Two Dimensional Wave Tank, *China Ocean Engineering*, **18**(4): 551 ~ 566.

Shu, K. D., Choi, J. C., Kim, B. H., Park, W. S. and Lee, K. S., 2001. Reflection of irregular waves from perforated-wall caisson breakwaters, *Coastal Engineering*, **44**(2): 141 ~ 151.